Available online at www.sciencedirect.com
SCIENCE DIRECT®
Journal of Solid State Chemistry 177 (2004) 824–833
JOURNAL OF SOLID STATE CHEMISTRY
http://elsevier.com/locate/jssc

Deuterium diffusion in vanadium deuterides (VD_x; $0.4 \leqslant x \leqslant 0.6$) studied by ^2H NMR

Shigenobu Hayashi*

Institute for Materials and Chemical Process, National Institute of Advanced Industrial Science and Technology (AIST), Tsukuba Central 5, 1-1-1 Higashi, Tsukuba, Ibaraki 305-8565, Japan

Received 13 July 2003; received in revised form 8 September 2003; accepted 17 September 2003

Abstract

Sites and dynamics of deuterium in $VD_{0.50}$ as well as in $VD_{0.40}$ and $VD_{0.57}$ have been studied by means of X-ray diffraction, differential scanning calorimetry and ^2H NMR. $VD_{0.40}$ consists of the body-centered-cubic (*bcc*) α_D and body-centered-tetragonal (*bct*) β_D phases at room temperature and only the octahedral (O) sites are occupied in the β_D phase. On the other hand, in $VD_{0.50}$, consisting of the *bct* β_D phase at room temperature, the O site is dominantly occupied with a small occupancy of the tetrahedral (T) sites in the β_D phase. $VD_{0.57}$ is composed of the *bcc* α'_D (a high-deuterium-concentration phase of the α_D phase) and *bct* β_D phases at room temperature, and the occupancy of the T sites is observed. The mean activation energy (E_D) of the deuterium diffusion is much larger for the O sites than for the T sites, and the diffusion is also much slower in the O sites. The mean E_D values for the O sites are almost the same in the β_D phase of $VD_{0.40}$ and $VD_{0.50}$, although the distribution of the mean residence time is much larger in $VD_{0.50}$ than in $VD_{0.40}$.

Keywords: Hydrogen absorbing material; Metal hydride; Diffusion; Nuclear magnetic resonance (NMR)

1. Introduction

Metal hydrides are attractive as hydrogen-storage materials. Materials with high hydrogen capacity are desirable for practical applications. Vanadium (V) metal can absorb a large amount of hydrogen to the extent of a hydrogen-to-metal atomic ratio of 2 [1]. The structures and phase diagrams of vanadium hydrides have extensively been studied so far, including vanadium deuterides, and it is well known that there are large isotope effects between the VH_x and VD_x systems [1].

H and D occupy different sites in the monohydride phase ($x \approx 1$) of vanadium, resulting in much different phase diagrams between the V–H and V–D systems [1]. For example, at room temperature, $VH_{0.8}$ has a body-centered-tetragonal (*bct*) structure with H atoms occupying octahedral (O) sites, which is referred as the ζ_H phase. $VH_{0.5}$ has also the *bct* structure. On the other hand, $VD_{0.8}$ has a body-centered-cubic (*bcc*) structure in which most of D atoms occupy tetrahedral (T) sites. The interstitial D atoms form an ordered orthorhombic sublattice below about 230 K, while above 230 K the D atoms distribute randomly. Those phases are denoted as δ_D and α_D (or α'_D) below and above 230 K, respectively. On the other hand, $VD_{0.5}$ has a *bct* structure different from that of $VD_{0.8}$, and D atoms occupy the O sites predominantly. Thus, in the V–D system the crystal structure and the deuterium site are dependent on the D concentration markedly in contrast to the V–H system.

Nuclear magnetic resonance (NMR) is useful to study hydrogen diffusion in metal hydrides. Fukai and Kazama have studied hydrogen diffusion in VH_x ($0.49 \leqslant x \leqslant 0.74$) by ^1H NMR [2]. The observed anomalous temperature dependence of ^1H spin–lattice relaxation time (T_1) was explained as a consequence of temperature-dependent activation energy of hydrogen diffusion. We have studied hydrogen diffusion in $VH_{0.59}$ and $VH_{0.77}$, relating it to the superstructures of H atoms [3,4]. On the other hand, ^2H NMR has been applied to vanadium deuterides to study the deuterium sites in the lattice [5,6]. Salibi et al., have studied ^2H relaxation behavior in vanadium deuterides [7]. The results of $VD_{0.59}$ were complicated, and thus further

*Corresponding author. Fax: +81-298-61-4515.
E-mail address: hayashi.s@aist.go.jp.

0022-4596/$ - see front matter © 2003 Elsevier Inc. All rights reserved.
doi:10.1016/j.jssc.2003.09.015

measurements were necessary to elucidate the deuterium diffusion at this deuterium concentration. We also studied the isotope effect on hydrogen (and deuterium) diffusion in the V–H–D systems with the ([H]+[D])/[V] ratio of about 0.8 [8,9]. The effects of Ti addition to V on hydrogen diffusion have been studied for Ti–V–H–D systems [10–18].

Although many studies have been performed for vanadium hydrides and deuterides up to now, the deuterium diffusion around $VD_{0.5}$ is not understood well. As described above, $VD_{0.5}$ has a *bct* structure similar to $VH_{0.5}$, and the O sites are occupied predominantly in both $VD_{0.5}$ and $VH_{0.5}$ [1]. To our knowledge, deuterium diffusion in the O sites has not been reported so far, except for the V–H–D and Ti–V–H–D systems which contain H and D simultaneously [8,9,16–18].

In the present work, we have studied V–D systems with the [D]/[V] ratios of 0.4–0.6. $VD_{0.5}$ has a crystal structure different from $VD_{0.8}$, as described above. The site occupancies and the crystal structures depend on the [D]/[V] ratio, and then the deuterium diffusion is expected to depend on the [D]/[V] ratio. We report the results of X-ray powder diffraction (XRD), differential scanning calorimetry (DSC) and ^{2}H NMR, and discuss on the sites and diffusion of deuterium. We also discuss the isotope effect in the diffusion of H or D atoms in the O sites.

2. Experimental

2.1. Materials

Vanadium metal powder (325 mesh, 99.5% min) was obtained from Mitsuwa Pure Chemicals (Japan). The deuteride samples were prepared by a reaction between the vanadium metal and D_2 gas at pressures less than 0.1 MPa in a glass vacuum line with a calibrated inner volume. The metal powder of about 2 g was first outgassed at 1073 K in a quartz tube by evacuation with a rotary vacuum pump (about 10^{-1} Pa) and then held at 773 K, where a required amount of D_2 gas was introduced. The temperature of the quartz tube containing the metal powder was gradually decreased to ambient temperature, spending time longer than 5 h. The D content was determined from the volume of the absorbed D_2 gas within the error of ± 0.02 [8]. The compositions of the synthesized samples were $VD_{0.40}$, $VD_{0.50}$ and $VD_{0.57}$.

2.2. X-ray diffraction and thermal analysis

XRD patterns were measured by a Rigaku MiniFlex diffractometer with Cu$K\alpha$ radiation at room temperature. DSC was measured by Rigaku Thermo Plus DSC 8230 in an N_2 atmosphere. The sample temperature was cycled in the range between 150 and 434 K. The temperature was decreased first, then increased and finally decreased at a rate of 5 K min^{-1}.

2.3. NMR measurements

The ^{2}H NMR measurements were performed by Bruker ASX200 and MSL400 spectrometers. Larmor frequencies were 30.7 and 61.4 MHz for ASX200 and MSL400, respectively. The 90° pulse widths were 4–6 μs at 30.7 MHz and 3.5–7 μs at 61.4 MHz, which were determined for each sample at several temperatures.

The spectra were measured with the quadrupole echo pulse sequence ($90°_x$–τ_1–$90°_y$–τ_2–echo). The τ_1 value was set at 15 μs, and τ_2 was adjusted to the echo maximum. The frequency scale of the spectra was referenced to the signal of D_2O.

The inversion recovery pulse sequence followed by the quadrupole echo pulse sequence ($180°-\tau-90°_x-\tau_1-90°_y-\tau_2-$echo) was used for most of the T_1 measurements. The saturation recovery method was used below about 300 K at 30.7 and 61.4 MHz for $VD_{0.40}$ and below about 270 K at 30.7 MHz for $VD_{0.50}$. The pulse sequence was $(90°-\tau_3)_n-\tau-90°_x-\tau_1-90°_y-\tau_2-$echo, where τ denoted the variable delay time and τ_1, τ_2 and τ_3 were fixed delay times. In both pulse sequences the τ_1 value was set at 15 μs and τ_2 was adjusted to the echo maximum. The values of τ_3 and n were 20 μs and 10 at 30.7 MHz and 30 μs and 7 at 61.4 MHz, respectively. The magnetization was first saturated by a string of 90° pulses, and then its recovery with time was monitored.

The sample temperature was corrected by separately measuring the signals of deuterated methanol under the same conditions [19]. The corrected temperature was used throughout this work.

3. Results and discussion

3.1. X-ray powder diffraction

Fig. 1 shows XRD patterns. The patterns can be interpreted as consisting of two structures, *bcc* and *bct*. The determined lattice constants are listed in Table 1.

The $VD_{0.50}$ sample consists of the *bct* structure, which is ascribed to the β_D phase [1]. Diffraction peaks are observed at 40.4° (indexed as (101)), 42.4° (110), 55.6° (002), 61.5° (200), 72.4° (112), 76.2° (211) and 87.3° (202).

The *bct* β_D phase is dominant in $VD_{0.40}$, although a small amount of a *bcc* phase coexists. The *bcc* phase is ascribed to the α_D phase [1], which gives diffraction peaks at 41.9° (110) and 61.1° (200), similarly to vanadium metal [3].

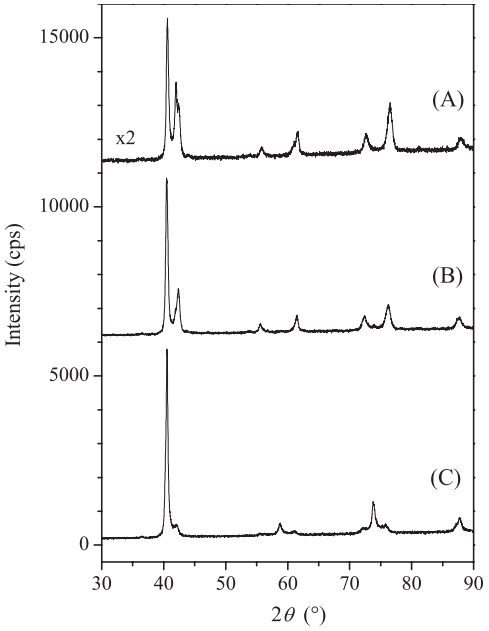

Fig. 1. XRD patterns of (A) $VD_{0.40}$, (B) $VD_{0.50}$, and (C) $VD_{0.57}$ at room temperature. The zero lines of the pattern are shifted arbitrarily.

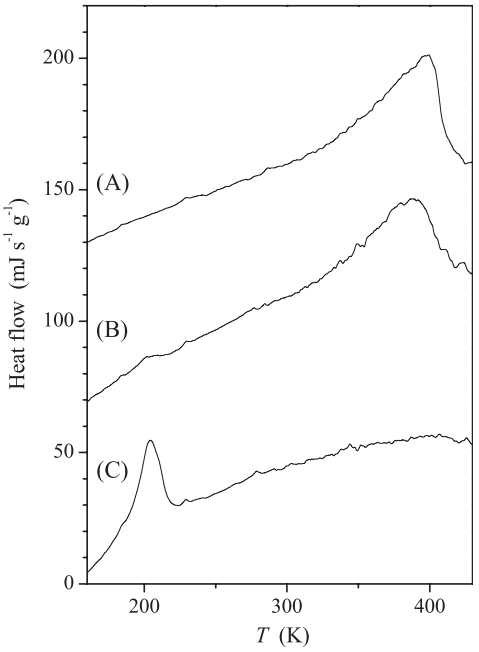

Fig. 2. DSC curves of (A) $VD_{0.40}$, (B) $VD_{0.50}$, and (C) $VD_{0.57}$. Heat absorption is expressed as the positive direction. The magnitudes of the heat flow are normalized by the sample weight, and the zero positions are shifted by arbitrary amounts.

Table 1
Crystal structures

Sample	*bcc*	*bct*	
	a_0 (nm)	a_0 (nm)	c_0 (nm)
$VD_{0.40}$[a]	0.304	0.301	0.329
$VD_{0.50}$		0.302	0.331
$VD_{0.57}$[b]	0.315	0.303	0.331
$VD_{0.81}$[c]	0.316		

[a] The *bct* phase is dominant while *bcc* is minor.
[b] The *bcc* phase is dominant with a small amount of *bct*.
[c] Ref. [8].

On the other hand, a *bcc* phase is dominant in $VD_{0.57}$, producing diffraction peaks at 40.5° (110), 58.7° (200), 73.8° (211) and 87.7° (220). This *bcc* phase is named α'_D phase in this work to differentiate from the α_D phase in $VH_{0.40}$, though α_D phase was sometimes used in both cases [1]. The α_D phase and the α'_D phase are much different in their deuterium concentration around room temperature and, therefore, their lattice constants are also much different from each other, as shown in Table 1. The $VD_{0.57}$ sample also contains a small amount of the *bct* β_D phase.

3.2. DSC

Fig. 2 shows a part of the DSC curves, which are measured with increasing temperature. Endothermic peaks are observed when the temperature increases. The numerical results are summarized in Table 2. The higher-end temperature, T_H, agrees with the reported phase boundary [1], and it is insensitive to the direction of temperature change and the sample. Therefore, T_H is used in the following discussion.

The $VD_{0.40}$ sample consists of the α_D and β_D phases at room temperature [1], as confirmed by the X-ray diffraction. The phase transition at 410 K is ascribed to that from $(\alpha_D + \beta_D)$ to α_D [1]. The similar phase transition at 413 K in $VD_{0.50}$ corresponds to that from β_D to α_D [1]. The $VD_{0.57}$ sample consists of the α'_D and β_D phases at room temperature [1], as confirmed also by the X-ray diffraction, and the phase transition at 217 K is that from $(\beta_D + \delta_D)$ to $(\alpha'_D + \beta_D)$ [1]. A similar phase transition from δ_D to α'_D was observed at 240 K for $VD_{0.81}$ consisting of only the α'_D phase at room temperature [8].

The $VD_{0.50}$ sample shows another small endothermic peak at 214 K. This might suggest that the $VD_{0.50}$ sample contains a small amount of the *bcc* α'_D (or δ_D) phase, because the transition temperature agrees with that from δ_D to α'_D in $VD_{0.57}$. However, the ΔH values in Table 2 suggest that the amount of the *bcc* phase is much less than 5%, because $VD_{0.57}$ consists of the *bcc* and *bct* phases. Indeed, we could not confirm the presence of the *bcc* phase in the $VD_{0.50}$ sample by the X-ray diffraction, although a negligible amount might be present.

3.3. ^2H NMR spectra

^2H NMR spectra have been recorded at 30.7 and 61.4 MHz. Figs. 3–5 show several typical ^2H NMR

Table 2
Results of DSC measurements

Sample	Temperature change	T_L[a] (K)	T_M[b] (K)	T_H[c] (K)	ΔH[d] (J g^{-1})
$VD_{0.40}$	Up	330±10	399±2	410±5	−24
	Down	304±10	372±2	411±5	+19
$VD_{0.50}$	Up	190±5	202±2	214±5	−0.4
		325±10	388±3	413±5	−18
	Down	304±10	390±3	414±5	+16
		NC[e]	185±5	217±5	NC[e]
$VD_{0.57}$	Up	172±5	204±2	217±3	−8
	Down	NC[e]	201±2	215±3	NC[e]
$VD_{0.81}$[f]	Up	200±5	228±3	240±5	

[a] The lower-end temperature.
[b] The temperature of the peak.
[c] The higher-end temperature.
[d] Heat flow.
[e] Not clear.
[f] Ref. [8].

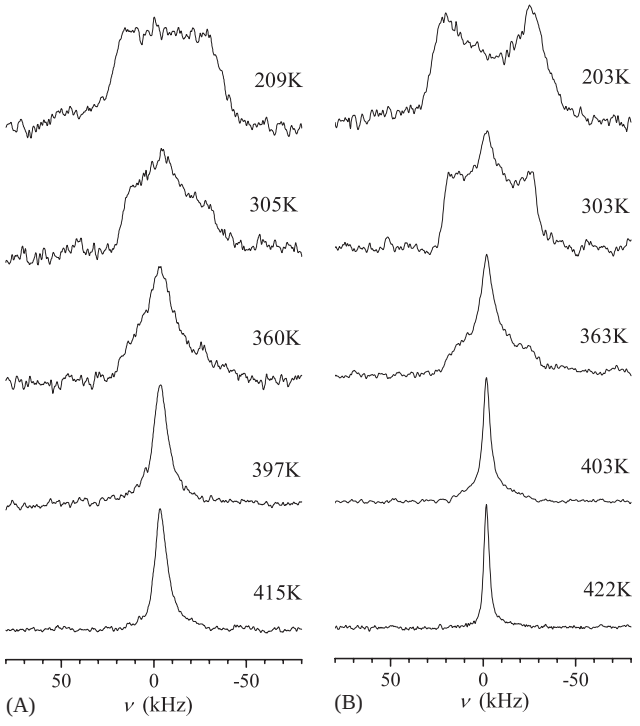

Fig. 3. Temperature dependence of ^{2}H NMR spectra in $VD_{0.40}$, measured at (A) 61.4 MHz and (B) 30.7 MHz.

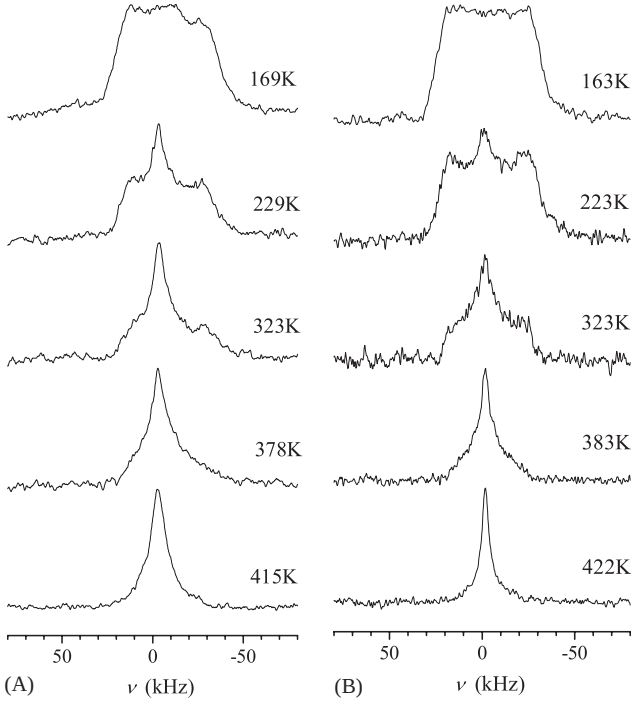

Fig. 4. Temperature dependence of ^{2}H NMR spectra in $VD_{0.50}$, measured at (A) 61.4 MHz and (B) 30.7 MHz.

spectra of $VD_{0.40}$, $VD_{0.50}$ and $VD_{0.57}$, respectively. The spectral line shape depends on temperature, reflecting the diffusion mode.

The spectra measured at the lowest temperatures are regarded as those in an almost rigid state. Two spectra measured at 61.4 and 30.7 MHz for each sample are simulated together using the same adjustable parameters with consideration of ^{2}H quadrupole and Knight shift interactions simultaneously [20], as has been carried out previously [8]. The asymmetry factor of the Knight shift interaction and three Euler angles defining the relative orientation of the two interactions are assumed to be 0. The simulated results are shown in Figs. 6–8.

The following parameters are obtained for $VD_{0.40}$ from the simulation shown in Fig. 6; QCC (quadrupole coupling constant, e^2Qq/h) = 70 kHz, η_Q (asymmetry factor) = 0.1, K_{iso} (isotropic Knight shift) = −24 ppm from D_2O and ΔK (magnitude of Knight shift anisotropy) = 260 ppm. These parameters demonstrate that deuterium occupies the O site in the β_D site [8], because the coexisting α_D phase has a very small D concentration [1]. The absence of a hollow in the central part of the

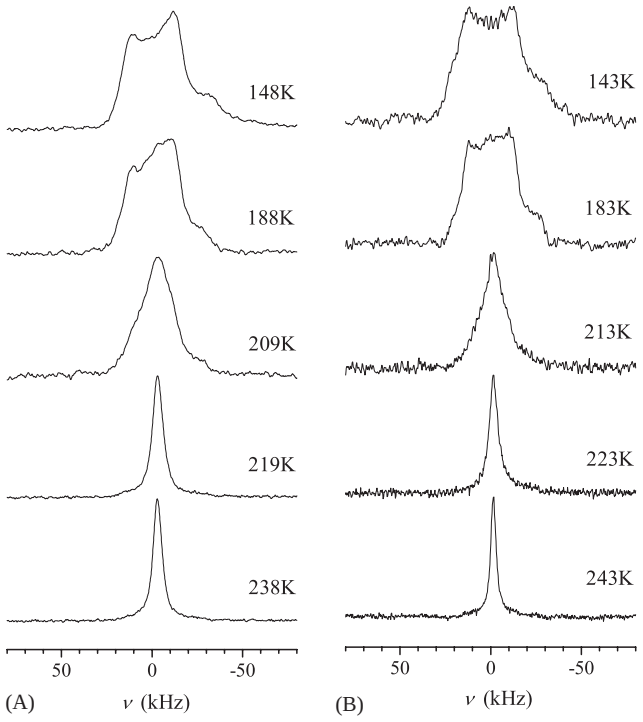

Fig. 5. Temperature dependence of ^{2}H NMR spectra in $VD_{0.57}$, measured at (A) 61.4 MHz and (B) 30.7 MHz.

spectra at 209 K and at 61.4 MHz (Fig. 6(A)) suggests that D atoms already start to diffuse at this temperature. With increase in temperature, a peak grows up in the central part of the spectra, as shown in Fig. 3. A narrow central peak is clearly observed at about 260 K, though the outer doublet remains up to about 340 K. Above 340 K, the doublet peak disappears, though a broad signal is observed at the bottom of the narrow central peak up to about 410 K. Thus, D atoms are located at the O sites and diffuse rather anisotropically in the β_D phase. Above 410 K only the narrow central peak is observed, indicating that the D diffusion becomes isotropic. The DSC results indicate that a phase transition from ($\alpha_D + \beta_D$) to α_D takes place at 410 K. In the α_D phase D atoms occupy the T sites [1] and the diffusion is isotropic.

As for $VD_{0.50}$, the simulation of the spectra at about 160 K, shown in Fig. 7, gives the following parameters; QCC = 64 kHz, $\eta_Q = 0.1$, $K_{iso} = -30$ ppm and $\Delta K = 250$ ppm. These values demonstrate that the O sites are occupied dominantly [8], although the values of QCC and ΔK are a little smaller than those for $VD_{0.40}$. The absence of a hollow in the central part of the observed spectra (Figs. 7(A) and (C)) suggests that a part of D atoms starts to diffuse at about 160 K. Although the temperature dependence of the line shape is similar to that in $VD_{0.40}$, the following differences are observed. With increase in temperature, a narrow central peak appears clearly at about 210 K, which is much low than the temperature for $VD_{0.40}$. This narrow

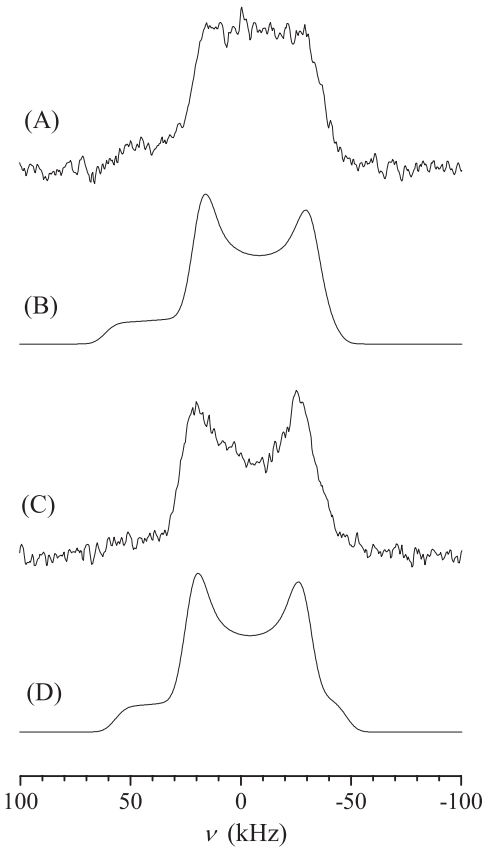

Fig. 6. ^{2}H NMR spectra of $VD_{0.40}$ measured (A) at 209 K and 61.4 MHz and (C) at 203 K and 30.7 MHz, and (B, D) their respective simulated spectra.

central peak is ascribed to D atoms occupying the T sites, as will be described in the ^{2}H T_1 section. The area of the narrow central peak is about 9% of the total, which is much larger than that predicted from the amount of the *bcc* α'_D (or δ_D) phase in the DSC results (much less than 5%). Thus, most of the T sites are included in the *bct* β_D phase. Some literatures said that about 5% of D atoms occupy the T sites in the β_D phase [1]. Above 260 K, D atoms in the O sites also contribute to the narrow central peak, as in the case of $VD_{0.40}$. Above 420 K the narrow central peak becomes dominant, although a small amount of a broad signal might remain at the bottom. The DSC results indicate that a phase transition from β_D to α_D takes place at 413 K.

The spectra of $VD_{0.57}$ at about 140 K can be simulated by a component with QCC = 38 kHz, $\eta_Q = 0.1$, $K_{iso} = -41$ ppm and $\Delta K = -130$ ppm. These parameters demonstrate that the T sites are occupied [8]. D atoms occupy the ordered T sites at low temperatures, and the ordering remains up to about 200 K. The ordered D sublattice is collapsed by the phase transition from the δ_D phase to the α'_D phase, accompanied by the growth of the narrow central line. After the phase transition, the doublet disappears, and only the narrow central line is observed, reflecting the isotropic nature of D diffusion. The doublet begins to collapse at 210 K,

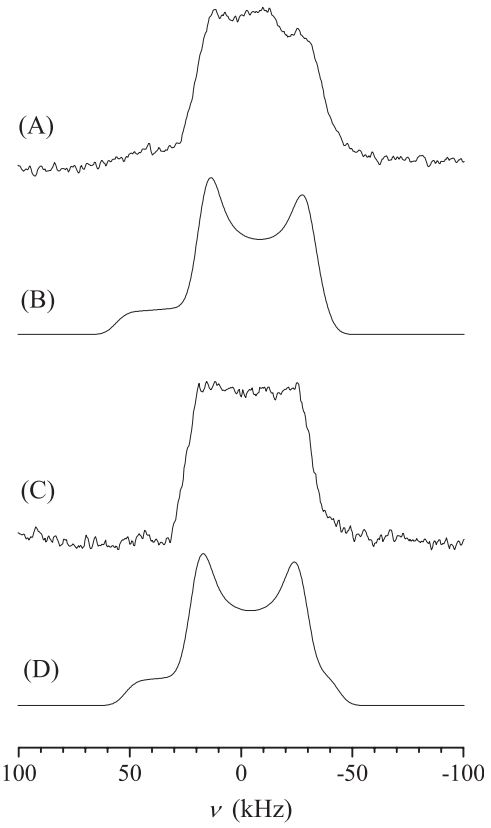

Fig. 7. ^{2}H NMR spectra of $VD_{0.50}$ measured (A) at 169 K and 61.4 MHz and (C) at 163 K and 30.7 MHz, and (B, D) their respective simulated spectra.

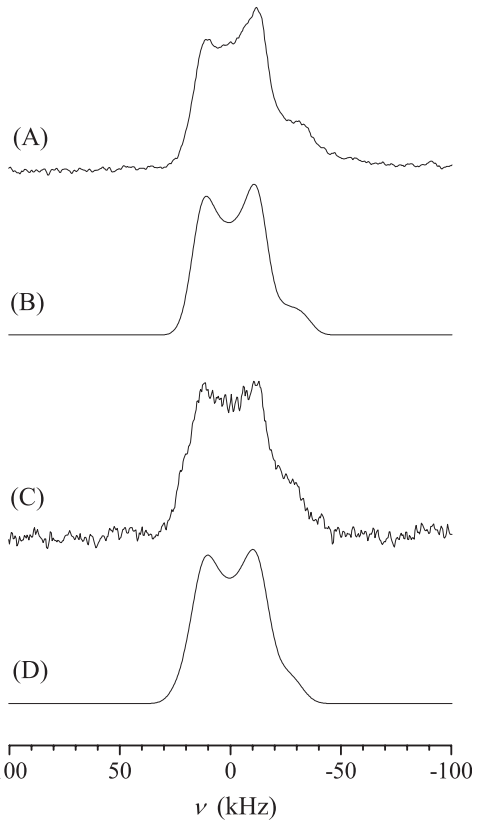

Fig. 8. ^{2}H NMR spectra of $VD_{0.57}$ measured (A) at 148 K and 61.4 MHz and (C) at 143 K and 30.7 MHz, and (B, D) their respective simulated spectra.

and the narrowing completes at 220 K. These temperatures agree with the DSC results. Note that occupancy of the O sites is not confirmed from the ^{2}H NMR spectra although the X-ray diffraction results indicate that the *bct* phase is contained.

In summary, the O sites are occupied dominantly in the β_D phase of $VD_{0.40}$ (below 410 K) and $VD_{0.50}$ (below 413 K), while the T sites are occupied in the δ_D and α'_D phases of $VD_{0.57}$. At most 9% of the D atoms occupy the T sites in the β_D phase of $VD_{0.50}$.

3.4. ^{2}H spin–lattice relaxation times

^{2}H spin–lattice relaxation times, T_1, have been measured at 30.7 and 61.4 MHz. The T_1 values are determined from the recovery of peak amplitudes in the Fourier-transformed (FT) spectra. At high temperatures, the ^{2}H resonance line shapes are narrow with only one prominent peak. Below certain temperatures, the resonance lines become broad and the line shapes have fine structures due to ^{2}H nuclear quadrupole interaction. In this case the relaxation curves are obtained at two positions; the left peak (i.e., the higher frequency side) of the doublet and the narrower central peak.

For $VD_{0.50}$, the relaxation curves obtained at the narrower central peak show non-exponential decays in a temperature range between 200 and 325 K. On the other hand, the curves obtained from the left peak of the doublet are exponential in the same temperature range. The doublet signal underlies the narrower central peak, and then it affects the relaxation curve obtained at the narrower central peak. By subtracting the contribution of the doublet signal, the T_1 values of the narrow central component are estimated. The relaxation curves are exponential outside the above temperature range. For $VD_{0.40}$ and $VD_{0.57}$, the two curves agree and always show exponential decays.

The spin–lattice relaxation times are plotted in Figs. 9–11 as a function of inverse temperature. For $VD_{0.40}$, there are minimum values of 0.16 s at about 360 K when measured at 30.7 MHz, while the minimum at 61.4 MHz is 0.33 s at about 380 K. The position of the minimum is just below the temperature of the phase transition, and thus the minimum is originated from the effect of the phase transition. The dominant component in the $VD_{0.50}$ sample has a minimum value of 0.19 and 0.38 s at about 380 K at 30.7 and 61.4 MHz, respectively. The phase transition causes the minimum in $VD_{0.50}$ also. The narrow central component in the $VD_{0.50}$ sample shows relatively short T_1 values in a temperature range between 200 and 325 K, and the temperature dependence and the magnitude of the T_1 values resemble those

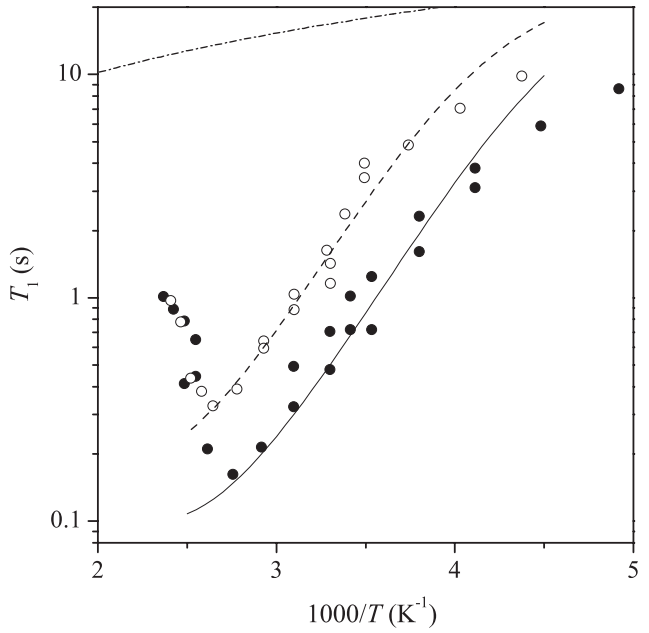

Fig. 9. ^{2}H spin–lattice relaxation times in $VD_{0.40}$ at 30.7 (●) and 61.4 MHz (○), and their simulated results indicated by the solid and chain lines. The chain–dotted line indicates the contribution of conduction electrons.

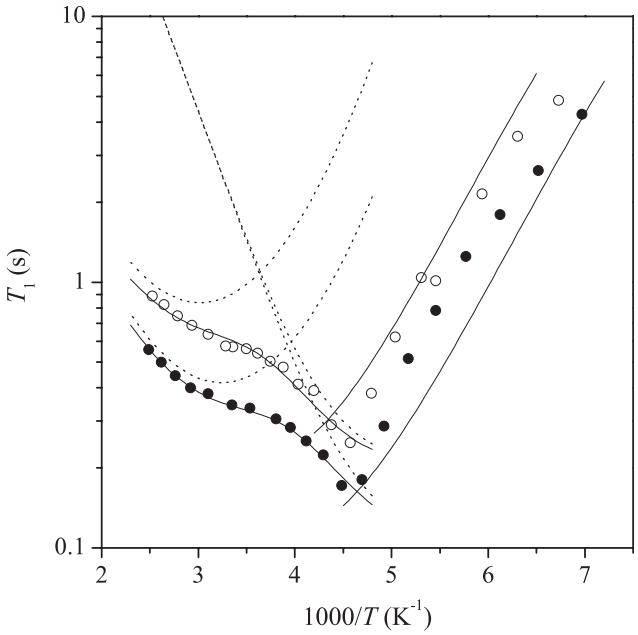

Fig. 11. ^{2}H spin–lattice relaxation times in $VD_{0.57}$ at 30.7 (•) and 61.4 MHz (○), and their simulated results indicated by the solid lines. The dotted lines indicate components used for the simulation in the high-temperature range.

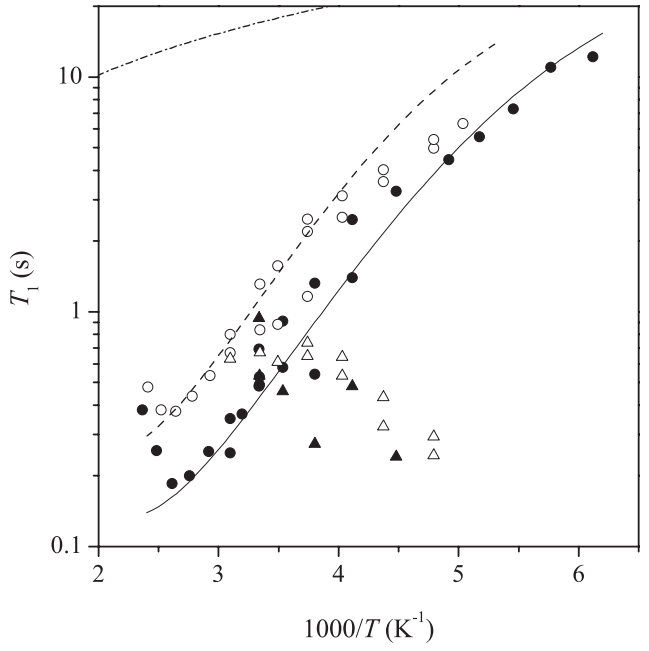

Fig. 10. ^{2}H spin–lattice relaxation times in $VD_{0.50}$ at 30.7 (●, ▲) and 61.4 MHz (○, △), and their simulated results indicated by the solid and chain lines. Circles correspond to the dominant component; the broad doublet signal and a narrow central peak below and above 325 K, respectively. Triangles correspond to the narrow central component in the temperature range between 200 and 325 K, from which the contribution of the dominant component was subtracted. The simulation was done for the dominant component. The chain–dotted line indicates the contribution of conduction electrons.

of $VD_{0.57}$ and $VD_{0.81}$ [8], where D atoms occupy the T sites. Consequently, this component in $VD_{0.50}$ is ascribed to the T sites. For $VD_{0.57}$, there is a minimum value of 0.17 and 0.25 s at about 220 K at 30.7 and 61.4 MHz, respectively. The phase transition again creates these minima. In $VD_{0.57}$, the parameters of deuterium diffusion change around the phase transition temperature and, moreover, it seems that there exist simultaneously more than one type of motions at high temperatures, similarly to $VD_{0.81}$ [8].

3.5. Analysis of ^{2}H spin–lattice relaxation times

The ^{2}H spin–lattice relaxation time in the present system is expressed as

$$(T_1)^{-1} = (T_{1q})^{-1} + (T_{1d})^{-1} + (T_{1e})^{-1}, \quad (1)$$

where $(T_{1q})^{-1}$ is contribution due to fluctuation of ^{2}H quadrupole interaction, $(T_{1d})^{-1}$ is contribution from nuclear dipolar interactions, $(T_{1e})^{-1}$ arises from the interaction with conduction electrons. The contribution of paramagnetic impurities is negligible in the samples of this work, similarly to the previous work [8]. The temperature dependence of T_{1e} is given by Korringa relation, $T_{1e}T = \text{constant}$. ^{2}H Korringa constants ($T_{1e}T$) are estimated from the respective ^{1}H Korringa constant multiplied by 42.44 ($= \gamma_H^2/\gamma_D^2$). The ^{1}H Korringa constants are assumed to be 120 s K from the values of the η_H phase [2], and the corresponding ^{2}H Korringa constants are listed in Table 3.

Table 3
^{2}H Korringa constants and parameters of D diffusion

Sample	$T_{1e}T$[a] (s K)	Site	τ_{0D}[a] (s)	E_D (kJ mol^{-1})	β_Q (kJ mol^{-1})	β_0	QCC (kHz)
$VD_{0.40}$	5100	O	13×10^{-14}	35	6	0	25
$VD_{0.50}$	5100	O	13×10^{-14}	36	10	0	25
$VD_{0.57}$	5100	T[b]	4.2×10^{-14}	23	4.5	0	25
		T[c]	4.2×10^{-14}	17	3.3[d]	0[d]	25[d]
		O′[c,e]	13×10^{-14}	26	0	3.2	15
$VD_{0.81}$[f]	6370	T[g]	4.2×10^{-14}	23.0	5.0	0	21
		T[h]	4.2×10^{-14}	17.5	3.8[d]	0[d]	21[d]
		O′[e,h]	13×10^{-14}	27.0	12.0	0	14

[a] Assumed.
[b] Below 210 K.
[c] Above 220 K.
[d] β_Q/E_D, β_0 and QCC are assumed to be the same as the lower-temperature values.
[e] The O site used as a diffusion path at the high-temperature range.
[f] Ref. [9].
[g] Below 220 K.
[h] Above 240 K.

The BPP-type equation for the quadrupole relaxation [21,22] is modified by assuming a log-normal distribution of mean residence times [23], as in the previous works [9,18]. The distribution of the mean residence time is considered to come from small displacements in the metal arrangement caused by neighboring hydrogen [18]. The quadrupole relaxation rate is described as

$$(T_{1q})^{-1} = \int F(S)\frac{3}{40}\left(\frac{e^2Qq}{\hbar}\right)^2\left(1+\frac{\eta_Q^2}{3}\right)\left[\frac{\tau_D}{1+(\omega_D\tau_D)^2}+\frac{4\tau_D}{1+(2\omega_D\tau_D)^2}\right]dS, \quad (2)$$

where ω_D and τ_D are the angular resonance frequency and the mean residence time of ^{2}H, respectively. The η_Q value is assumed to be zero. The function $F(S)$ is a distribution function

$$F(S) = \frac{1}{\beta_1\sqrt{\pi}}\exp\left(-\frac{S^2}{\beta_1^2}\right), \quad (3)$$

$$S = \ln\frac{\tau_D}{\tau_{mD}}, \quad (4)$$

$$\beta_1^2 = \beta_0^2 + \left(\frac{\beta_Q}{RT}\right)^2, \quad (5)$$

and

$$\tau_{mD} = \tau_{0D}\exp\left(\frac{E_D}{RT}\right). \quad (6)$$

The symbol of τ_{0D} is the mean residence time at the infinite temperature, E_D is the activation energy, and R is the gas constant. The symbols of β_0 and β_Q are parameters defining the magnitude of the distribution. They relate to the distributions of the pre-exponential factor and the activation energy centered by τ_{0D} and E_D, respectively. The distribution with $\beta_0 = 0$ has been applied to V–Nb–H and V–Ta–H(D) systems [24,25].

The dipolar contribution in Eq. (1) is written as [21,22]

$$(T_{1d})^{-1} = \int F(S)M_{DV}\left[\frac{0.5\tau_D}{1+\{(1-\gamma_V/\gamma_D)\omega_D\tau_D\}^2}+\frac{1.5\tau_D}{1+(\omega_D\tau_D)^2}+\frac{3\tau_D}{1+\{(1+\gamma_V/\gamma_D)\omega_D\tau_D\}^2}\right]dS. \quad (7)$$

In the above equation M_{DV} are the second moments given by [22]

$$M_{DV} = \frac{4}{15}\gamma_D^2\gamma_V^2\hbar^2 I_V(I_V+1)\sum_j r_j^{-6}. \quad (8)$$

The symbols of γ_D and γ_V are gyromagnetic ratios of ^{2}H and ^{51}V spins, respectively, $\hbar$ is Planck constant, and r_j is a distance between ^{2}H and ^{51}V spins. The symbol I_V is a nuclear spin quantum number of ^{51}V, which is 7/2.

Because the dipolar relaxations in both ^{1}H and ^{2}H spins are dominated by the dipolar interaction with ^{51}V spins, the ratio of relaxation rates scales roughly γ_H^2/γ_D^2. The $VH_{0.82}$ sample shows ^{1}H T_1 minimum values of 8.0 and 15 ms at 30.3 and 59.8 MHz, respectively, in which the O sites are occupied similarly to $VD_{0.50}$ [8]. The expected ^{2}H T_1 minimum values caused by the dipolar interaction are calculated as 0.34 and 0.64 s at the corresponding frequencies. The experimental ^{2}H T_1 minimum values for $VD_{0.50}$ are 0.19 and 0.38 s at 30.7 and 61.4 MHz, respectively. These comparisons between the scaled ^{1}H T_1 and the experimental ^{2}H T_1 show that the quadrupole interaction contributes to the ^{2}H spin–lattice relaxation.

The dipolar relaxation shows temperature and frequency dependences similar to those of the quadrupole

relaxation. Only the quadrupole relaxation described by Eq. (2) is taken into account in the simulation. The parameter of the quadrupole coupling constant includes the contribution from the dipolar interaction, if it contributes.

The simulated results are shown in Figs. 9–11 by chain and solid lines. Similarly to the previous works [8,9,14–18], the τ_{0D} values are assumed to be 13×10^{-14} and 4.2×10^{-14} s for the O and T sites, respectively, from the relation that $\tau_{0D} = 1.4\tau_{0H}$. This relation is originated from the different masses of H and D. The obtained parameters are listed in Table 3.

3.6. Sites and dynamics of D

$VD_{0.40}$ consists of the *bcc* α_D and *bct* β_D phases at room temperature. Only the O sites are occupied in the β_D phase, as revealed by the ^2H NMR spectra. On the other hand, in $VD_{0.50}$, consisting of the *bct* β_D phase at room temperature, the O site is dominantly occupied with a small occupancy of the T sites in the β_D phase. $VD_{0.57}$ is composed of the *bcc* α'_D and *bct* β_D phases at room temperature. The ^2H NMR spectra of $VD_{0.57}$ demonstrate that the T sites are occupied and there are no evidences of the occupancy of the O sites in the low-temperature phases, the *bcc* δ_D and *bct* β_D phases. The β_D-phase region in the phase diagram covers the range between $VD_{0.45}$ and $VD_{0.55}$ at room temperature [1]. The T sites are not occupied at the phase boundary of the low D concentration side, and the occupancy of the T sites increases as the D concentration increases.

The temperature dependence of the spectral line shapes indicates that D jumps among ordered sites predominantly in the β_D and δ_D phases, whereas in the α_D and α'_D phases D jumps among disordered sites. Jumps among ordered sites lead to incomplete narrowing due to anisotropy of the motion. On the other hand, jumps among disordered sites average the quadrupole interaction as well as the anisotropy of the Knight shift interaction completely. The mean residence times are plotted in Figs. 12 and 13. They are calculated using the parameters in Table 3. The mean E_D values for the O sites are almost the same in the β_D phase of $VD_{0.40}$ and $VD_{0.50}$, although the distribution of the mean residence time is much larger in $VD_{0.50}$ than in $VD_{0.40}$. The simultaneous occupancy of the O and T sites in $VD_{0.50}$ might increase the distribution. The mean activation energy is much smaller for the T sites than for the O sites, and the diffusion is also much faster in the T sites. The phase transition from δ_D to α'_D in $VD_{0.57}$ increases the diffusion rate in the T sites. In the α'_D phase of $VD_{0.57}$, the O sites are considered to be used as a diffusion path. The O site occupancy of 7% or 10% was reported in the α'_D phase [1].

The activation energy (E_D) for the O sites is $36.0\,kJ\,mol^{-1}$ in $VD_{0.50}$. This is larger than those for

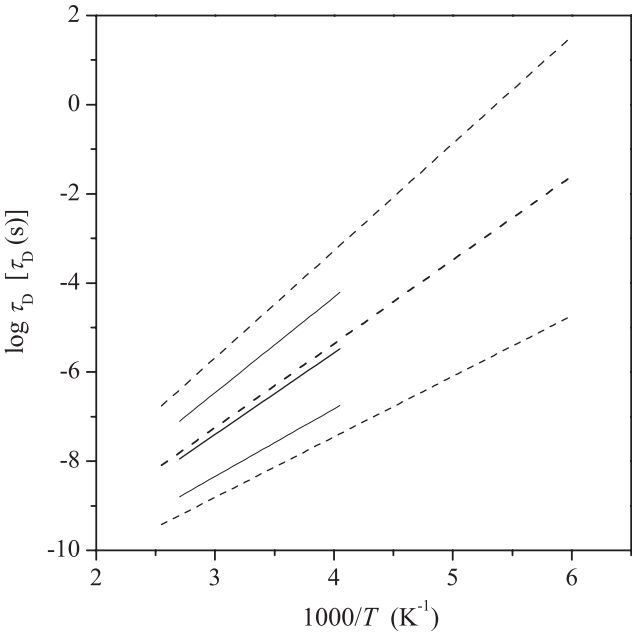

Fig. 12. The distribution of the mean residence times for $VD_{0.40}$ (solid lines) and $VD_{0.50}$ (chain lines). The three lines correspond to the mean residence times at $S = +\beta_1$, 0, $-\beta_1$.

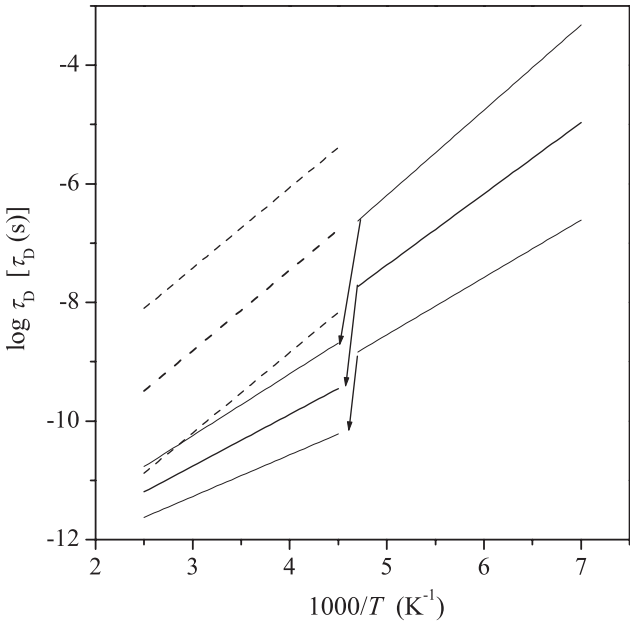

Fig. 13. The distribution of the mean residence times for $VD_{0.57}$. The solid and chain lines correspond to the T sites and the O sites, respectively. The three lines correspond to the mean residence times at $S = +\beta_1$, 0, $-\beta_1$. The arrows indicate the changes due to the phase transition.

the O sites in $VH_{0.82}$ ($E_H = 27.0\,kJ\,mol^{-1}$) and $VH_{0.60}D_{0.20}$ ($E_H = 25.0\,kJ\,mol^{-1}$, $E_D = 28.0\,kJ\,mol^{-1}$) [9]. It has been reported that the decrease in the hydrogen concentration increases the activation energy in the β_H phase [2,26]. For example, Fukai and Kazama reported E_H values of 40 and $28\,kJ\,mol^{-1}$ for $VH_{0.486}$,

and $VH_{0.736}$, respectively, although the analysis method was much different [2]. Bowman et al. also reported a value of $40\,kJ\,mol^{-1}$ for $VH_{0.50}$ [27]. The similar mechanism can be applied to the β_D phase of VD_x as follows. When $x \leqslant 0.5$ in VD_x, only the O_{z1} sites are occupied and the O_{z2} sites are empty. With increase in x, the O_{z2} sites are partially occupied and provide an easier diffusion pathway.

The activation energy is larger in D than in H for $x \sim 0.8$ [8,9]. However, for $x \sim 0.50$, the activation energy is larger in H ($E_H = 40\,kJ\,mol^{-1}$) than in D ($E_D = 36.0\,kJ\,mol^{-1}$). Bowman et al. reported a value of $30\,kJ\,mol^{-1}$ for $VT_{0.50}$ [27]. The present value for $VD_{0.50}$ lies between those of $VH_{0.50}$ and $VT_{0.50}$. Thus, the activation energies are in the order H > D > tritium. This is an inverse isotope effect, because heavier isotopes generally diffuse more slowly. This unusual isotope effect might be explained by the mechanism proposed by Bowman et al. [26]. In their mechanism, H atoms occupy only the O_{z1} sites in $VH_{0.50}$. On the other hand, other octahedral sites (O_{z2}, O_x and O_y) and the T sites are partially occupied in $VT_{0.50}$, although the O_{z1} sites are dominantly occupied. The disordered occupancy might decrease the activation energy. Actually, the T site occupancy is observed in $VD_{0.50}$. The degree of the disordered occupancy is considered to be in the following increasing order; $VH_{0.50} < VD_{0.50} < VT_{0.50}$.

4. Conclusions

$VD_{0.50}$, together with $VD_{0.40}$ and $VD_{0.57}$, has been studied by means of X-ray diffraction, DSC and ^2H NMR, and the following conclusions have been obtained.

(1) $VD_{0.40}$ consists of the *bcc* α_D and *bct* β_D phases at room temperature and only the O sites are occupied in the β_D phase. On the other hand, in $VD_{0.50}$, consisting of the *bct* β_D phase at room temperature, the O site is dominantly occupied with a small occupancy of the T sites in the β_D phase. $VD_{0.57}$ is composed of the *bcc* α'_D and *bct* β_D phases at room temperature, and the T sites are occupied. Although the ^2H spectra do not show the occupancy of the O sites, the relaxation results suggest partial occupancy of the O sites in the α'_D phases.

(2) The mean activation energy of D diffusion is much larger for the O sites than for the T sites, and the diffusion rate is much slower in the O sites. The mean E_D values for the O sites are almost the same in the β_D phase of $VD_{0.40}$ and $VD_{0.50}$, although the distribution of the mean residence time is much larger in $VD_{0.50}$ than in $VD_{0.40}$.

Acknowledgments

This study was financially supported by the Budget for Nuclear Research of the Ministry of Education, Culture, Sports, Science and Technology, based on the screening and counseling by the Atomic Energy Commission.

References

[1] T. Schober, H. Wenzl, in: G. Alefeld, J. Völkl (Eds.), Hydrogen in Metals, Vol. 2, Springer, Berlin, 1978, p. 11.
[2] Y. Fukai, S. Kazama, Acta Metall. 25 (1978) 11.
[3] S. Hayashi, K. Hayamizu, O. Yamamoto, J. Chem. Phys. 76 (1982) 4392.
[4] S. Hayashi, K. Hayamizu, O. Yamamoto, J. Chem. Phys. 77 (1982) 2210.
[5] K. Nakamura, Bull. Chem. Soc. Jpn. 46 (1973) 2588.
[6] R.R. Arons, H.G. Bohn, H. Lutgemeier, J. Phys. Chem. Solids 35 (1974) 207.
[7] N. Salibi, B. Ting, D. Cornell, R.E. Norberg, Phys. Rev. B 38 (1988) 4416.
[8] B. Bandyopadhyay, S. Hayashi, Phys. Rev. B 60 (1999) 10302.
[9] S. Hayashi, J. Phys. Chem. Solids 64 (2003) 2227.
[10] S. Hayashi, K. Hayamizu, O. Yamamoto, J. Solid State Chem. 46 (1983) 306.
[11] S. Hayashi, K. Hayamizu, O. Yamamoto, J. Chem. Phys. 78 (1983) 5096.
[12] S. Hayashi, K. Hayamizu, J. Less-Common Met. 161 (1990) 61.
[13] T. Ueda, S. Hayashi, K. Hayamizu, Phys. Rev. B 48 (1993) 5837.
[14] T. Ueda, S. Hayashi, J. Alloys Compds. 231 (1995) 226.
[15] T. Ueda, S. Hayashi, J. Alloys Compds. 256 (1997) 145.
[16] B. Bandyopadhyay, S. Hayashi, J. Alloys Compds. 305 (2000) 136.
[17] B. Bandyopadhyay, S. Hayashi, J. Alloys Compds. 330–332 (2002) 443.
[18] S. Hayashi, J. Solid State Chem. 170 (2003) 82.
[19] A.L. Van Geet, Anal. Chem. 40 (1968) 2227.
[20] S. Hayashi, Magn. Reson. Chem. 34 (1996) 791.
[21] N. Bloembergen, E.M. Purcell, R.V. Pound, Phys. Rev. 73 (1948) 679.
[22] A. Abragam, The Principles of Nuclear Magnetism, Oxford University Press, London, 1961.
[23] E.R. Andrew, D.J. Bryant, E.M. Cashell, Chem. Phys. Lett. 69 (1980) 551.
[24] L. Lichty, J. Shinar, R.G. Barnes, D.R. Torgeson, D.T. Peterson, Phys. Rev. Lett. 55 (1985) 2895.
[25] A.V. Skripov, M.Yu. Belyaev, A.P. Stepanov, L.N. Padurets, E.I. Sokolova, J. Alloys Compds. 190 (1993) 171.
[26] R.C. Bowman Jr., in: G. Bambakidis (Ed.), Metal Hydrides, Plenum, New York, 1981, p. 109.
[27] R.C. Bowman Jr., A. Attalla, B.D. Craft, Scr. Metall. 17 (1983) 937.